

*Rapid communication***Influence of laser fluence and irradiation timing of F<sub>2</sub> laser on ablation properties of fused silica in F<sub>2</sub>–KrF excimer laser multi-wavelength excitation process**K. Obata<sup>1,2,\*</sup>, K. Sugioka<sup>1</sup>, T. Akane<sup>1</sup>, N. Aoki<sup>1,2</sup>, K. Toyoda<sup>2</sup>, K. Midorikawa<sup>1</sup><sup>1</sup>RIKEN (The Institute of Physical and Chemical Research), Hirosawa 2-1, Wako, Saitama 351-0198, Japan<sup>2</sup>Department of Applied Electronics, Science University of Tokyo, Yamazaki 2641, Noda, Chiba 278-8510, Japan

Received: 16 July 2001/Accepted: 27 July 2001/Published online: 2 October 2001 – © Springer-Verlag 2001

**Abstract.** A collinear irradiation system of F<sub>2</sub> and KrF excimer lasers for high-quality and high-efficiency ablation of hard materials by the F<sub>2</sub> and KrF excimer lasers' multi-wavelength excitation process has been developed. This system achieves well-defined micropatterning of fused silica with little thermal influence and little debris deposition. In addition, the dependence of ablation rate on various conditions such as laser fluence, irradiation timing of each laser beam, and pulse number is examined to investigate the role of the F<sub>2</sub> laser in this process. The multi-wavelength excitation effect is strongly affected by the irradiation timing, and an extremely high ablation rate of over 30 nm/pulse is obtained between –10 ns and 10 ns of the delay time of F<sub>2</sub> laser irradiation. The KrF excimer laser ablation threshold decreases and its effective absorption coefficient increases with increasing F<sub>2</sub> laser fluence. Moreover, the ablation rate shows a linear increase with the logarithm of KrF excimer laser fluence when the F<sub>2</sub> laser is simultaneously irradiated, while single KrF excimer laser ablation shows a nonlinear increase. The ablation mechanism is discussed based on these results.

**PACS:** 42.62.-b; 42.70.Ce; 81.65.Cf

Fused silica is widely used not only in optoelectronics but also in various other fields such as micromechanics and microchip chemistry. However, precision microfabrication of fused silica is quite difficult due to its excellent properties of high transmittance in a wide wavelength range and high chemical stability. Recently, ablation using a vacuum ultraviolet (VUV) laser has become a candidate precision microfabrication tool of fused silica [1, 2]. However, the VUV laser has some drawbacks for practical use, i.e. high photon cost, unreliability, instability, and small pulse energy. In order to overcome these problems, we have developed a VUV–UV multi-wavelength excitation process in which a VUV laser beam with small fluence is simultaneously introduced to conventional UV laser ablation [3, 4]. The multi-wavelength ex-

citation process has many advantages over single-wavelength ablation using the VUV laser: (i) the small fluence of the VUV laser in the former process reduces the photon cost of the high-fluence VUV laser in the latter process; (ii) therefore, the processing area and throughput increase; (iii) additionally, since ablation proceeds via the UV laser beam, the necessity for expensive VUV optics and projection systems is eliminated; (iv) finally, variation in the ablation quality as a result of VUV laser pulse-to-pulse energy instability and spatial uniformity is minimized. In the early stage, we used a VUV Raman laser as the light source of VUV and UV lasers [5, 6]. The use of the VUV Raman laser enabled high-quality ablation of various hard materials such as fused silica, GaN, and SiC [7]. However, the VUV Raman laser is unsuitable for practical use, since it simultaneously radiates 15 different wavelengths in the VUV to visible range and its pulse energy in the VUV region is too small, although it is a very attractive and effective system for fundamental research. Therefore, in order to apply this technique in practical use, we developed a new tool for the multi-wavelength excitation process by simultaneous irradiation by F<sub>2</sub> and KrF excimer lasers [8]. In that stage, the F<sub>2</sub> laser was irradiated from the back of the fused silica. This process achieved high-quality ablation similar to single-wavelength ablation using a F<sub>2</sub> laser, as well as that by the multi-wavelength excitation process using a VUV Raman laser. However, irradiation by the F<sub>2</sub> laser from the back of the sample brings about some disadvantages. Namely, most of the F<sub>2</sub> laser energy is absorbed by the fused silica during its transmission to the front surface and cannot contribute to the multi-wavelength excitation process. Furthermore, this scheme cannot be used for the ablation of other materials with strong absorption of the F<sub>2</sub> laser, such as GaN and SiC.

In this study, we developed a new collinear irradiation system of F<sub>2</sub> and KrF excimer lasers which yields an effective multi-wavelength excitation process. In addition, characterization of this process under various conditions of laser fluence, irradiation timing of each laser beam, and pulse number was carried out, which had not yet been conducted in detail. The role of the F<sub>2</sub> laser in this process is discussed based on the results obtained.

\*Corresponding author.

(Fax: +81-48/468-4682, E-mail: kobata@postman.riken.go.jp)

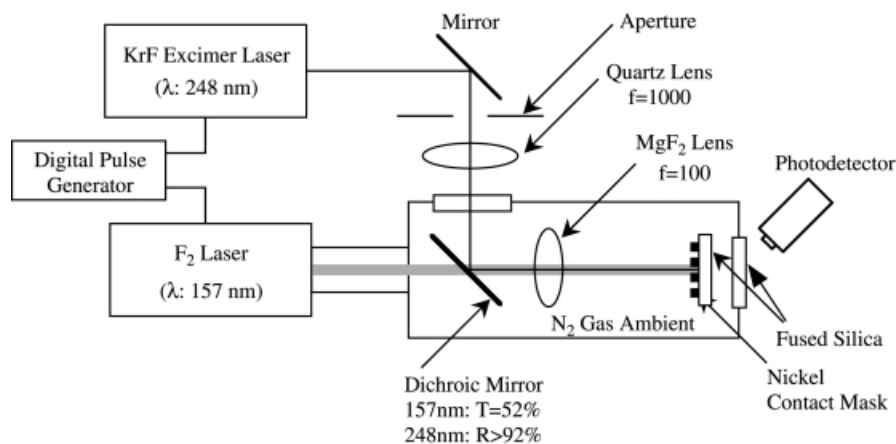
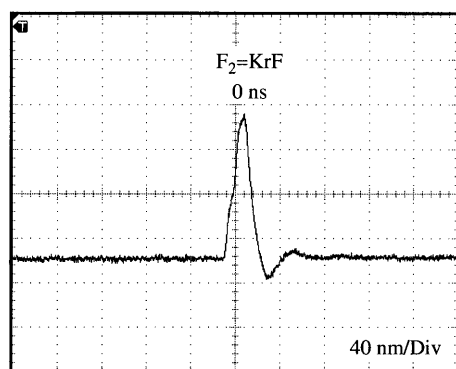


**Fig. 1.** Schematic illustration of experimental setup for a multi-wavelength excitation process of collinear irradiation by  $F_2$  and KrF excimer lasers

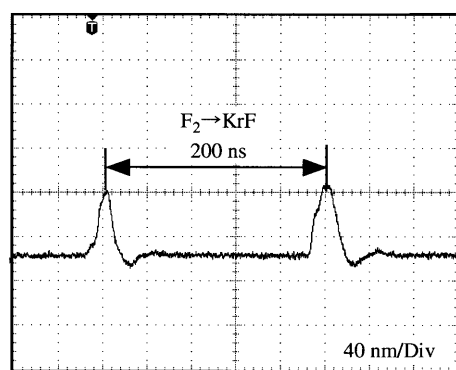
## 1 Experimental procedure

A schematic illustration of the experimental setup for ablation by simultaneous irradiation using  $F_2$  and KrF excimer lasers is shown in Fig. 1. UV-grade fused-silica (VIOSIL, thickness of 0.525 mm, Shin-Etsu Chemical Co. Ltd.) substrates were used in this experiment. The fused-silica substrates were ultrasonically cleaned with acetone and ethanol, followed by a deionized water for 5 min. Then, the fused-silica substrate was placed into the chamber. The chamber was filled with dry nitrogen gas at 1 atm to prevent absorption of the  $F_2$  laser beam by oxygen. The fused-silica substrates were ablated by

$F_2$  ( $\lambda = 157$  nm,  $\tau = 20$  ns) and KrF excimer ( $\lambda = 248$  nm,  $\tau = 23$  ns) lasers. For collinear irradiation by  $F_2$  and KrF excimer laser beams, a dichroic mirror, which was composed of multi-layers of dielectric thin films on a  $MgF_2$  substrate, was used. This mirror transmits 52% of the  $F_2$  laser beam and reflects more than 92% of the KrF excimer laser beam. To detect each laser pulse at the sample surface, fluorescence from the fused silica was observed by a photodetector, and then the irradiation timing of each beam was adjusted by a digital pulse generator (Stanford DG 535). Figure 2 shows the photodetector spectra adjusted for (a) simultaneous irradiation and (b)  $F_2$  laser irradiation followed by KrF excimer laser irradiation with a 200-ns delay. In this setup, the controllability of the irradiation timing was about 1 ns. The repetition rate of both  $F_2$  and KrF excimer lasers was kept constant at 1 Hz to avoid the accumulation of heat induced by laser irradiation. The number of pulses was set at 10, except in the experiments on pulse-number dependence. Both of the laser beams behind the dichroic mirror were focused by a  $MgF_2$  lens onto the fused silica through a contact nickel mesh mask (array of  $30 \times 30 \mu m^2$ ). Ablated patterns were observed by atomic force microscopy (AFM). The etched depth was measured using a surface profiler ( $\alpha$ -Step: KLA Tencor Co. Ltd.).



**a**



**b**

**Fig. 2a,b.** Pulse-shape spectra of  $F_2$  and KrF excimer lasers simultaneously irradiated (a) and with a 200-ns delay time between irradiation by  $F_2$  and KrF excimer lasers (b)

## 2 Results and discussion

Figure 3 shows AFM images of fused silica ablated by (a) simultaneous irradiation by  $F_2$  and KrF excimer lasers and (b) irradiation by only the KrF excimer laser. The fluences of  $F_2$  and KrF excimer lasers are 0.23 and 4.0 J/cm<sup>2</sup>, respectively. The AFM image of the sample ablated by the multi-wavelength excitation process shows a well-defined pattern corresponding to the mask pattern. In addition, sharp edges and flat side walls were fabricated. A periodic ripple structure was formed on the bottom of the ablated area, which was deduced to have been fabricated by diffraction of the KrF excimer laser beam at the edges of the contact mask. Therefore, the ablated structure strongly reflects the spatial energy distribution of the laser beam, indicating little thermal influence. On the other hand, the AFM image of the fused silica ablated by only the KrF excimer laser shows irregular roughness at the bottom and swelling at the edges. Thus, simultaneous irradiation by the  $F_2$  laser beam with small laser fluence sig-

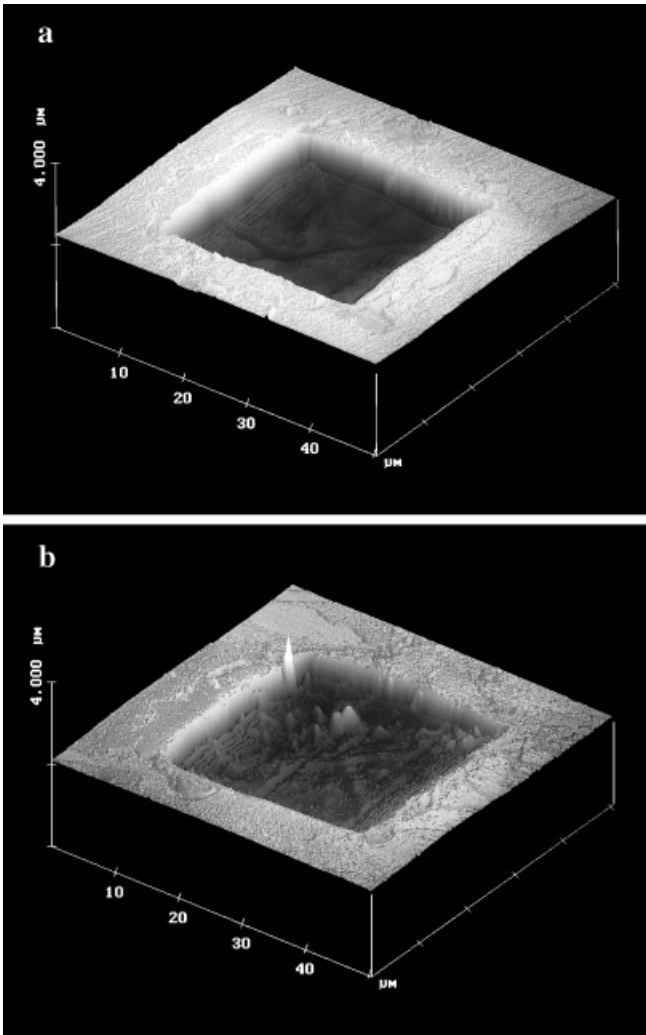


**Fig. 3a,b.** The AFM images of fused silica ablated by a multi-wavelength excitation process using  $F_2$  and KrF excimer lasers (a) and by irradiation by a single wavelength of the KrF excimer laser (b)

nificantly improved the ablation quality of fused silica to be almost comparable with that of single-wavelength ablation using a  $F_2$  laser as well as a VUV Raman laser [4].

The great improvement of ablation quality by the multi-wavelength excitation process is attributed to excited-state absorption (ESA). The ESA mechanism has previously been explained using the band structure of the fused silica [2, 6]. Here, it is briefly reviewed. Fused silica has a band gap of approximately 9.0 eV. Direct excitation of electrons from the valence band to the conduction band by the  $F_2$  laser is impossible, because the photon energy of 7.9 eV of the  $F_2$  laser is lower than the band gap. However, fused silica has many defect levels ascribed to defects and impurities below the conduction band. In fact, the absorption edge of the fused silica used in this study is approximately 170 nm, which corresponds to 7.3 eV. Therefore, the  $F_2$  laser beam can excite the electrons to the defect levels. The electrons trapped at these defect levels can be further excited to beyond the vacuum level by the KrF excimer laser beam, since the electron affinity (0.9 eV) of fused silica is much lower than the photon energy (5.0 eV) of the KrF excimer laser. This cascade excitation process based on ESA induces photoionization of

constituent atoms in fused silica and finally leads to photoinduced ablation. This ESA has been confirmed elsewhere by comparison of the pulse form of the KrF excimer laser beam transmitted by fused silica with and without  $F_2$  laser irradiation [8].

In order to achieve high-quality ablation of fused silica by the multi-wavelength excitation process, the irradiation timing of  $F_2$  and KrF excimer lasers is one of the most important factors. Figure 4 shows the variation of ablation rate as a function of the delay time of  $F_2$  laser irradiation after KrF excimer laser irradiation. A negative delay time corresponds to  $F_2$  laser irradiation followed by KrF excimer laser irradiation. In this experiment, the laser fluences of  $F_2$  and KrF excimer lasers are 0.4 and 2.9 J/cm<sup>2</sup>, respectively. An extremely high ablation rate of over 30 nm/pulse is achieved within a delay time of  $\pm 10$  ns. Therefore, multi-wavelength excitation is the most effective in this region. The relaxation rate of excited electrons in fused silica has been evaluated to be as short as 1.7 ns, which is less than the delay-time range (20 ns) [6]. One of the reasons is the long pulse durations of 20 ns (FWHM) for the  $F_2$  laser and 23 ns (FWHM) for the KrF excimer laser. Another reason may be the jitter of each pulse ( $\sim \pm 10$  ns). On the other hand, ablation with a rate as low as  $\sim 5$  nm/pulse takes place during the delay time from  $-500$  to  $-100$  ns. This ablation may be caused by electrons trapped at a different kind of defect level possessing a longer relaxation rate.

Another important factor for achieving high-quality ablation is the fluence of the  $F_2$  laser. Figure 5 shows the variation

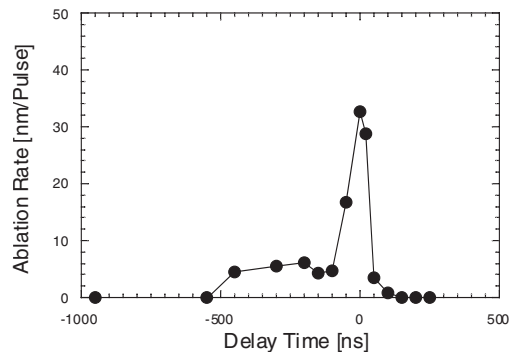


**Fig. 4.** Variation of ablation rate as a function of delay time of  $F_2$  laser irradiation after KrF excimer laser irradiation. The  $F_2$  and KrF excimer laser fluences were 0.4 J/cm<sup>2</sup> and 2.9 J/cm<sup>2</sup>, respectively

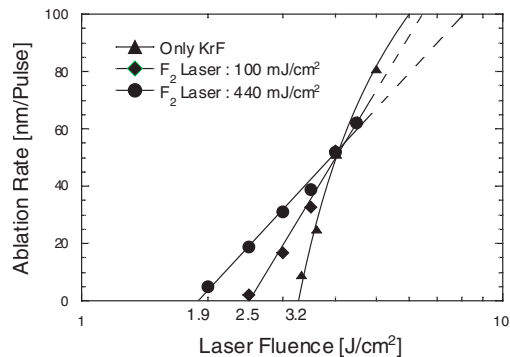


**Fig. 5.** Variation of ablation rate as a function of KrF excimer laser fluence with  $F_2$  laser fluences of 0, 100, and 440 mJ/cm<sup>2</sup>

of the ablation rate of fused silica as a function of the KrF excimer laser fluence for various  $F_2$  laser fluences (0, 100, and 440  $\text{mJ}/\text{cm}^2$ ) with the delay time of 0 ns. The ablation rates for the simultaneously irradiated samples show a linear increase with the logarithm of the KrF excimer laser fluence, at least up to 4.5  $\text{J}/\text{cm}^2$ . It is well known that the relationship between ablation rate  $d$  and laser fluence  $F$  in the case of single-photon absorption is expressed by

$$d = 1/\alpha_{\text{eff}} \ln(F/F_{\text{th}}), \quad (1)$$

where  $\alpha_{\text{eff}}$  and  $F_{\text{th}}$  are the effective absorption coefficient and the ablation threshold laser fluence, respectively. Therefore, the linear increase of the ablation rate indicates that ablation is caused by the single-photon absorption process of the KrF excimer laser. These results support the ESA mechanism described above. Namely, a single photon of the KrF excimer laser is absorbed by a single electron trapped at defect levels by the  $F_2$  laser, which then excites the electron to beyond the vacuum level. On the other hand, the ablation rate shows a nonlinear increase in the case of irradiation by only the KrF excimer laser. This nonlinear increase is due to multi-photon absorption, since the KrF excimer laser beam is not absorbed by fused silica without simultaneous irradiation by the  $F_2$  laser. The ablation threshold of the simultaneously irradiated samples becomes smaller than that with only KrF excimer laser ablation, and decreases with increasing  $F_2$  laser fluence. By extrapolation, the ablation thresholds of the KrF excimer laser with simultaneous irradiation by the  $F_2$  laser at 100 and 440  $\text{mJ}/\text{cm}^2$  are estimated to be 2.5 and 1.9  $\text{J}/\text{cm}^2$ , respectively. The effective absorption coefficient is calculated to be  $1.47 \times 10^5 \text{ cm}^{-1}$  for a  $F_2$  laser fluence of 440  $\text{mJ}/\text{cm}^2$ , using (1). This large effective absorption coefficient has almost the same value as that for single-wavelength ablation with the  $F_2$  laser [1].

Figure 6 shows the variation of the ablation rate of fused silica as a function of  $F_2$  laser fluence for 10 pulses and the delay time of 0 ns. The fluence of the KrF excimer laser was set at 3.0  $\text{J}/\text{cm}^2$ , which is below the ablation threshold for KrF excimer laser ablation (see Fig. 5). Therefore, no ablation takes place with only KrF excimer laser irradiation. However, simultaneous irradiation by the  $F_2$  laser with only a small laser fluence induces significant ablation. In addition, the ablation rate increases with increasing  $F_2$  laser fluence. This is mainly attributed to an increase in the number of electrons ex-

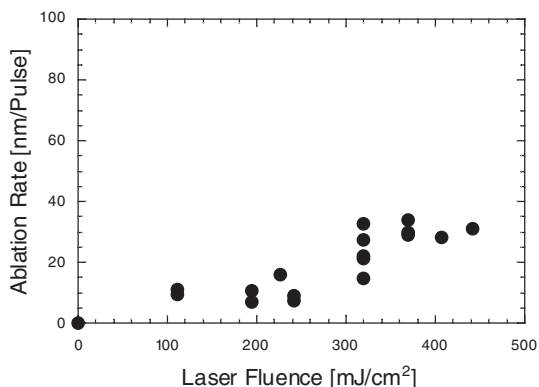


**Fig. 6.** Variation of ablation rate as a function of  $F_2$  laser fluence. The fluence of the KrF excimer laser was set at 3.0  $\text{J}/\text{cm}^2$

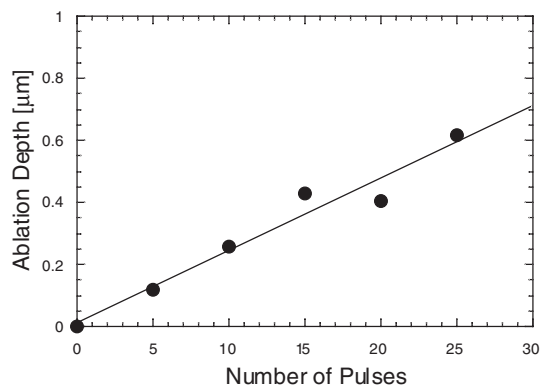


**Fig. 7.** Variation of ablation depth as a function of the number of laser pulses. The  $F_2$  and KrF excimer laser fluences were 0.23  $\text{J}/\text{cm}^2$  and 3.0  $\text{J}/\text{cm}^2$ , respectively

cited by the  $F_2$  laser, resulting in an increase of the absorption of the KrF excimer laser beam.

Figure 7 shows the variation of the ablation depth of fused silica ablated at 0.23  $\text{J}/\text{cm}^2$  of  $F_2$  laser fluence and 2.9  $\text{J}/\text{cm}^2$  of KrF excimer laser fluence with the delay time of 0 ns as a function of the number of pulses. The ablation depth shows a linear increase, indicating no incubation effect. This means that the ESA is the dominant mechanism in this process. The ablation rate is estimated to be as high as 23  $\text{nm}/\text{pulse}$ .

Thus, the multi-wavelength excitation process using simultaneous irradiation by  $F_2$  and KrF excimer lasers achieves high-quality and high-efficiency ablation of fused silica.

### 3 Conclusions

A multi-wavelength excitation process by collinear irradiation by  $F_2$  and KrF excimer lasers was developed. AFM images indicated that the simultaneous irradiation by the  $F_2$  and KrF excimer laser beams achieved high-quality ablation of fused silica. The ablation rate strongly depended on the irradiation timing of each laser beam, and an extremely high ablation rate of over 30  $\text{nm}/\text{pulse}$  was obtained within the delay time of  $\pm 10$  ns. The ablation rate of the simultaneously irradiated sample showed a linear increase with the logarithm of the KrF excimer laser fluence, which suggested single-photon absorption of the KrF excimer laser beam by electrons excited by  $F_2$  laser irradiation. On the other hand, the ablation rate of single-wavelength ablation using the KrF excimer laser showed a nonlinear increase due to multi-photon absorption. These results support the ESA mechanism in the multi-wavelength excitation process. The ablation threshold of the KrF excimer laser decreased and the effective absorption coefficient increased with increasing  $F_2$  laser fluence. Therefore, the  $F_2$  laser fluence, as well as the irradiation timing, is important in this process. The ablation depth increased linearly with increasing number of pulses, indicating that the ESA mechanism was dominant. Thus, we conclude that the multi-wavelength excitation process by collinear irradiation using  $F_2$  and KrF excimer lasers is promising for achieving high-quality and high-efficiency microfabrication of fused silica and enabling practical application.

*Acknowledgements.* The authors would like to thank K. Watanabe for his help with AFM observations and J. Zhang for helpful discussions on the experiment. K. Obata was supported by a grant from the Junior Research Associate (JRA) program of RIKEN.

## References

1. P.R. Herman, R.S. Marjoribanks, A. Oetli, K. Chen, I. Konovalov, S. Ness: *Appl. Surf. Sci.* **154–155**, 577 (2000)
2. P.R. Herman, B. Chen, D.J. Moore, M. Canaga-Reynam: *Mater. Res. Soc. Symp. Proc.* **236**, 52 (1992)
3. K. Sugioka, S. Wada, Y. Ohnuma, A. Nakamura, H. Tashiro, K. Toyoda: *Appl. Surf. Sci.* **96–98**, 347 (1996)
4. K. Sugioka, J. Zhang, S. Wada, H. Tashiro, K. Midorikawa: *Proc. SPIE* **3683**, 108 (1998)
5. K. Sugioka, S. Wada, A. Tsunemi, T. Sakai, H. Moriwaki, A. Nakamura, H. Tashiro, K. Toyoda: *Jpn. J. Appl. Phys.* **32**, 6185 (1993)
6. K. Sugioka, S. Wada, H. Tashiro, K. Toyoda, Y. Ohnuma, A. Nakamura: *Appl. Phys. Lett.* **67**, 2789 (1995)
7. J. Zhang, K. Sugioka, S. Wada, H. Tashiro, K. Toyoda, K. Midorikawa: *Appl. Surf. Sci.* **127–129**, 793 (1998)
8. J. Zhang, K. Sugioka, T. Takahashi, K. Toyoda, K. Midorikawa: *Appl. Phys. A* **71**, 23 (2000)